Acta Geodyn. Geomater., Vol. 21, No. 1 (213), 1–13, 2024
DOI: 10.13168/AGG.2024.0001
journal homepage: https://www.irsm.cas.cz/acta

ORIGINAL PAPER

CLUSTERED EROSIONAL SUBMARINE FURROWS AT BLAKE OUTER RIDGE ON THE U.S. ATLANTIC MARGIN: IMPLICATIONS FOR SPATIAL VARIATIONS OF THE DEEP WESTERN BOUNDARY CURRENT VELOCITY

Linfeng YUAN, Xuelu XIAO *, Xiaowei YANG , Longjian RAN and Huifang MING

722 Research Institute of China, State Shipbuilding Corporation Limited, Wuhan, China.

**Corresponding author's e-mail:* xiaoxuelu722@163.com

ARTICLE INFO

Article history:
Received 12 October 2023
Accepted 5 January 2024
Available 19 January 2024

Keywords:
Submarine furrows
Formation
Deep sea
Bottom currents
Deep Western Boundary Current
U.S. Atlantic margin

ABSTRACT

Based on multibeam bathymetric and seismic reflection data, morphology and depositional characteristics of the submarine furrows at the Blake Outer Ridge on the U.S. Atlantic margin were described in order to investigate the formation of the bedforms and estimate the spatial variations of the associated flow velocity. The furrows occur in clusters with an area of 83000 km^2 on the continental rise. Most of the furrows run parallel to isobaths at a water depth of 3000–5000 m and a few extend obliquely (~30°) to isobaths at a larger water depth. The furrows show an asymmetric V-shape on cross sections with a steeper wall on the upslope. They are 70–1100 m wide and 0.2–30 m deep. The furrow spacing varies between 145 m and 3045 m and ratios of furrow width to spacing are ~0.9 on average. As close to the furrowed field, the depositional layers thinned and truncations below the sea bed became more distinct. The furrows represent an erosional bedform, and the development of them has been governed by the behavior of the along-margin DWBC. During periods (e.g. glacial periods) when the DWBC is vigorous, the stronger bottom current eroded the seafloor by the secondary helical circulation in the bottom boundary layer and formed larger and more erosional furrows. During periods (e.g. interglacial periods) when the DWBC is weak, the weakened bottom current abraded the seafloor and formed smaller and less erosional furrows. It is inferred that the DWBC velocity gradually decreases along its path from 30 cm/s to 10 cm/s at the present. By contrast, the flow velocity had more than doubled through a bend and decreased by 1/3 across a large slump scar.

1. INTRODUCTION

Furrows are elongate sub-parallel longitudinal bedforms which form in fine – grained, cohesive sediments in variable environment, including deep seas, estuaries, and large lakes (Dyer, 1970; Flood 1981, 1983, 1994; Viekman et al., 1992; Canals et al., 2006; Biscara et al., 2010; Lobo et al., 2011). They are particularly abundant in the deep sea. Submarine furrows recorded the depositional processes and sedimentary history of both modern and ancient deep-sea environments (Flood, 1983; Poppe et al., 2002; Lastras et al., 2007; Biscara et al., 2010; Kilhams et al., 2011; Stow et al., 2013). Hence, a detailed research on submarine furrows could provide important information on changes of associated flows (Flood, 1994; Lobo et al., 2011; Rebesco et al., 2014).

Since the first description of furrows by Dyer (1970) and their identification in the deep sea (Lonsdale et al., 1973), submarine furrows have been observed in a number of areas by side-scan sonars, echo sounders, bottom cameras, 3.5 kHz chirp profiles, and seismic reflection data (McLean, 1981; Flood, 1983; Canals et al., 2006; Kilhams et al., 2011; Lobo et al., 2011). These researches have significantly improved our understandings of the distribution and formation of submarine furrows. Submarine furrows could occur individually or in groups on the continental margins (e.g. the shelf, slope, rise, and abyssal plain) and in the submarine canyons (Flood, 1983; Canal et al., 2006). Formation of submarine furrows may be related to the erosional and depositional processes of bottom currents (Flood, 1983; Stow et al., 2009), also be associated with erosion of turbidity currents flowing in the submarine canyons (Canals et al., 2006). Erosion and deposition in the submarine furrows could be induced by obstacle blocking (McLean, 1981) or the impact of the secondary flow at the bottom layer of bottom currents (Flood, 1981) and as well as the action of the flow filaments separated from the mean flow (Garcia et al. 2009). However, (1) few large fields of submarine furrows have been found, (2) origin and evolution of submarine furrows are still unclear to us, and (3) it urgently needs to find the qualitative relationship between furrow forms and the associated flows in order to reveal the changes of the flows and associated climate information.

In this study, we illustrated a large field of submarine furrows at the Blake Outer Ridge of the U.S. Atlantic margin, investigated origin and

Cite this article as: Yuan L, Xiao X, Yang X, Ran L, Ming H: Clustered erosional submarine furrows at the Blake Outer Ridge on the U.S. Atlantic margin: implications for spatial variations of the Deep Western Boundary Current velocity. Acta Geodyn. Geomater., 21, No. 1 (213), 1–13, 2024. DOI: 10.13168/AGG.2024.0001

development of these furrows, and explored bottom current behavior recorded by the furrows.

2. OCEANOGRAPHIC BACKGROUND

This study area is located at the Blake Outer Ridge just out of the continental shelf north of the Bahama Islands (Fig. 1). The Blake Outer Ridge is a sedimentary feature thought to have been formed by bottom currents (Jenkins and Rhines, 1980; Faugeres et al., 1999). Two major bottom currents influenced the study area, i.e. the Gulf Stream (Bryan, 1970; Phrampus and Hornbach, 2012) and the Deep Western Boundary Current (DWBC; Flood, 1994; Stahr and Sanford, 1999; Evans and Hall, 2008).

The Gulf Stream is an ocean current that modulates climate in the Northern Hemisphere by transporting warm waters from the Gulf of Mexico into the North Atlantic and Arctic oceans (Lynch-Stieglitz et al., 1999, 2011). The Gulf Stream flows north at water depths as great as ~1000 m. It has average volume transports of 30–32 Sv (1 Sv = 1×10^6 m^3/s) at the Blake Outer Ridge at the present (Lynch-Stieglitz et al., 1999). The Gulf Stream weakened during glacial periods (Lynch-Stieglitz et al., 1999).

The DWBC couples the global atmospheric climate to the ocean interior, making it an important component of the global climate system (Stahr and Sanford, 1999). This density-driven current flows south by transporting cold and heavy waters from the high-latitude region of the North Atlantic along the continental slope of the Western Atlantic to the Southern Ocean (Stahr and Sanford, 1999; Bras et al., 2017). The DWBC includes two types of water masses, i.e. the northern and southern components. The northern component includes the Labrador Sea water, Iceland-Scotland overflow water, and Denmark Strait overflow water (see review in Mosher et al. (2017) and Bras et al. (2017)). The southern component mainly consists of the Antarctic bottom water. The main body of the DWBC flows south at a water depth of ~2500–5000 m and a speed of 10–20 cm/s. It has volume transports of ~18 Sv at the Blake Outer Ridge at the present (Stahr and Sanford, 1999; Bras et al., 2017). During glacial periods, the core of the DWBC became shallower than the water depth of 2500 m (Oppo and Lehman, 1993; Franz and Tiedemann, 2002; Evans and Hall, 2008).

3. DATA AND METHODS

Data used in this study include multibeam bathymetric and three-dimensional multichannel seismic data.

The multibeam bathymetric data were downloaded from the National Geophysical Data Center (NGDC) database at the National Oceanic and Atmospheric Administration (NOAA) (http://www.ngdc.noaa.gov/mgg/bathymetry/multibeam.html) with the spatial resolution about 100 meters. The data cover our whole study area (Fig. 1). From the bathymetric data, basic morphometric parameters of submarine furrows, including widths, depths, spacing, and water depths, were measured.

The high-resolution three-dimensional multichannel seismic data were downloaded from the Opendtect website (http://opendtect.org/osr/). The open data have an area of over 370 km^2 in the southern Blake Outer Ridge, and covers the southern region of sediment wave fields (Fig. 1). The seismic data were collected during the fall of 2000 with bin sizes of 37.5 m in the inline direction and 75 m in the crossline direction (Hornbach et al., 2008). The dominant frequency of the seismic data ranges from 30 to 45 Hz. The corresponding vertical resolution (tuning thickness) varies between 14.2 to 9.5 m, assuming an average interval velocity of 1700 m/s for the near-seafloor interval. The seismic data revealed depositional and erosional characteristics of the submarine furrows.

4. RESULTS

4.1. DISTRIBUTION AND MORPHOLOGY OF THE SUBMARINE FURROWS

Submarine furrows are one of the most significant bedforms of the seabed at the Blake Outer Ridge. These furrows are distributed in clusters on the continental rise with a gradient of 0.43–0.62° in the region of 29.5–34° latitude and 72.4–76° longitude with an area of ~83000 km^2 (Figs. 1 and 2). Most of the furrows run roughly parallel to regional isobaths between water depths of 3000–5000 m, classified as type A (Figs. 1, 2 and 3). But some of the furrows extend 60–100 km obliquely to isobaths to ~30°at a water depth of ~5000 m before meeting the furrows of type A, classified as type B (Figs. 1, 2 and 3). The furrows show an asymmetric V shape of cross sections without flat trough floors and a slightly steeper wall on the upslope (Fig. 4). The furrows are 70–1100 m wide and 0.2–30 deep based on statistics of the twelve cross-section profiles (Table 1). The spacing of these furrows varies between 145–3045 m, and the ratio of width to spacing is 0.82–0.97 on average. The cross-section bathymetric profiles display that the furrows become smaller downslope. It is noted that the furrows of type B are significantly larger than those of type A although the former type occurs in the deeper water area (Fig. 4). The cross-section bathymetric profiles also show that furrow spacing and average width decrease toward the south from the location of the profile p1, then increase significantly and reach the maximum at the location of the profile p4 (Fig. 5). Further south, furrow spacing and average width decrease again. The twelve cross-section bathymetric profiles exhibit a fine linear proportional correlation of furrow widths and spacing with the average linear coefficient of 0.4 (Fig. 6).

Distinct morphologic differences occur between the furrowed field and outside. A group of at least eight submarine canyons/channels extended downslope to the north of this furrowed field. But no distinct

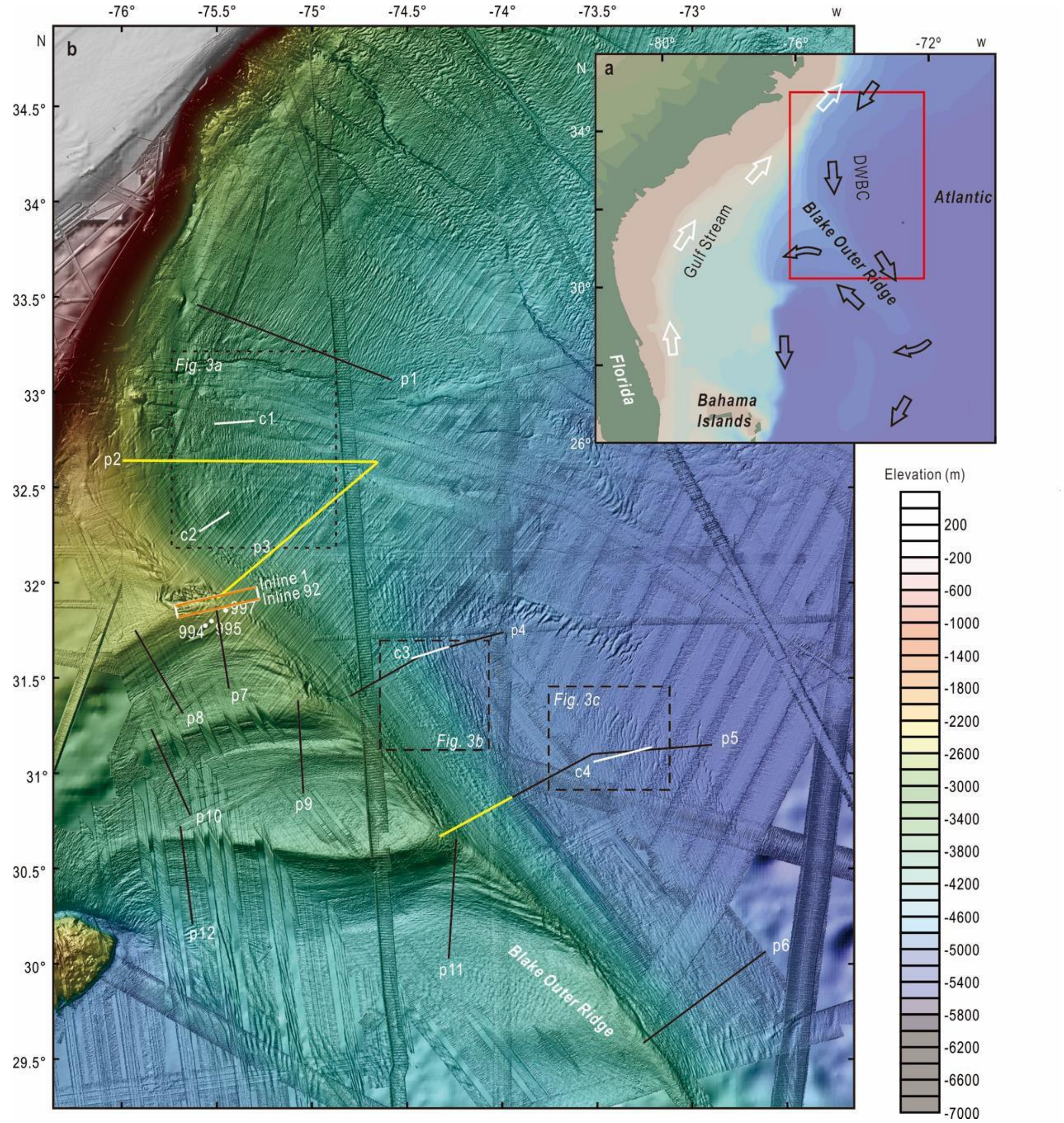

Fig. 1 Location of the study area (**a**) and its morphology (**b**). Red rectangle in (**a**) marks the region shown by (**b**). Black and white arrows in (**a**) respectively represent flow directions of the Gulf Stream and the DWBC. Black and white lines in (**b**) mark the locations of the cross-section bathymetric profiles. Yellow lines denote locations of the oceanographic measurements conducted by Stahr and Sanford (1999). The white rectangle in (**b**) marks the seismic survey location, and the orange lines represent the seismic profiles shown in this study. The black dotted rectangles denote the zones enlarged in Figure 3. The white dots mark the locations of ODP site 994, 995, 997.

submarine furrows have been found in the canyon-group area at the water depth range where the furrows appear (Fig. 2). Sediment waves exist in the shallower and deeper zones outside the furrowed field. The sediment waves grew on a gentle slope (0.15°–1.41°) at water depths of 2500–2850 m and ~5000 m and extended in a trend of northwest or northeast. The sediment waves have a wavelength of 1.0–1.8 km and a wave height of 16–110 m. Two large submarine slump scars, named the northern and southern scars, respectively, separated the furrow field into two parts (Fig. 2). The northern scar runs 145 km downslope from the water depth of ~3500 m to the water depth of ~4700 m with maximum width of 20 km and maximum relief of 50 m. It is located on the southern side of submarine canyon groups and marks the place where the furrows begin to extend along the continental rise (Fig. 2). The southern scar extends 180 km downslope from the water depth of ~3200 m to the water depth of ~5000 m with maximum width of 70 km and maximum relief of 130 m. No significant morphologic signs represent the growth of submarine furrows within the two failure zones (Fig. 2).

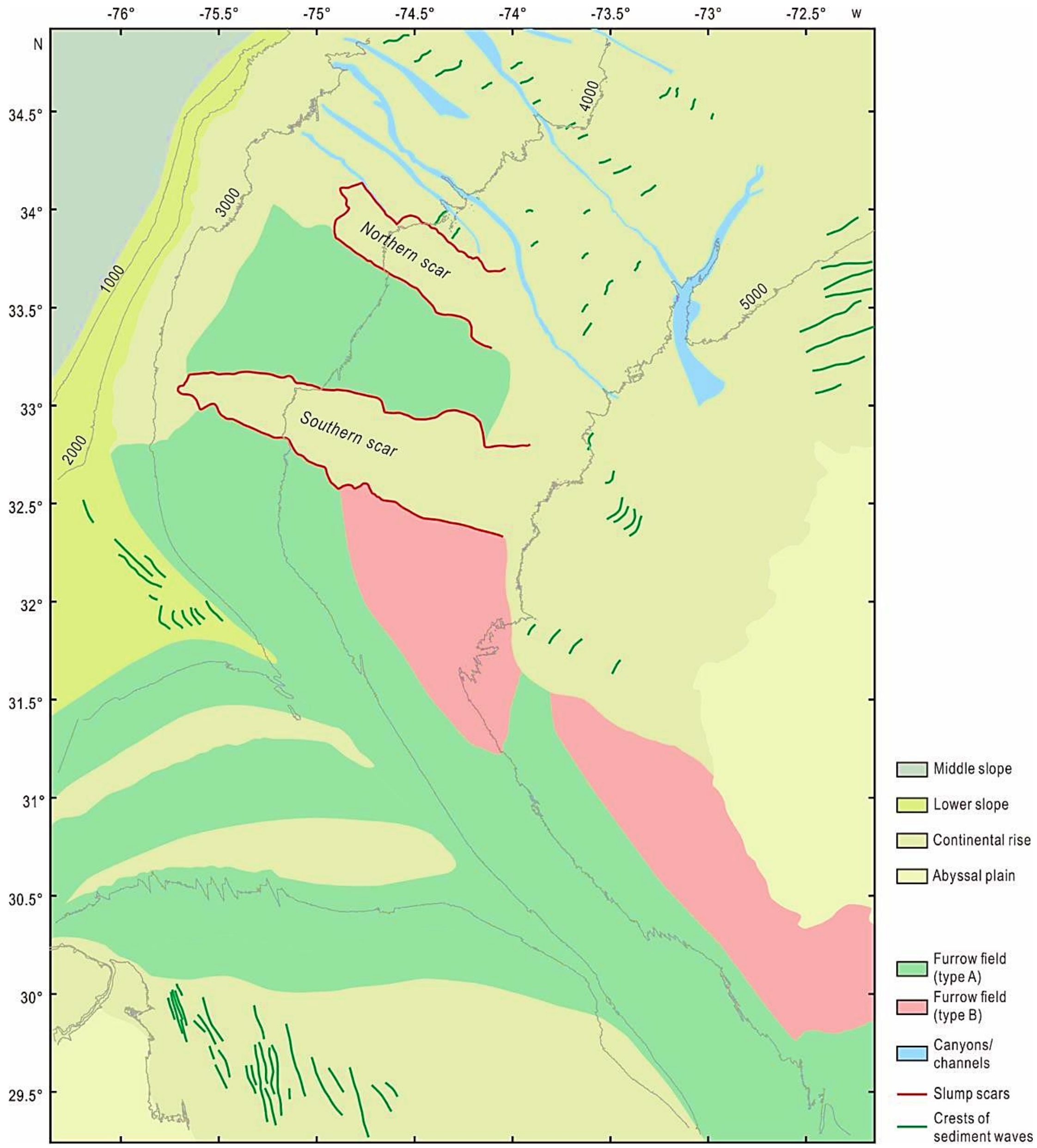

Fig. 2 Morphologic interpretation of the study area. The grey lines mark isobaths.

4.2. DEPOSITIONAL AND OCEANOGRAPHIC CHARACTERISTICS OF THE FURROWED FIELD

Seismic reflection data close to the western boundary of the furrowed field show depositional characteristics nearby this area. The data displayed more distinct truncations below the sea bed as close to the furrow filed. Upslope-migrating wavy seismic reflections appear to the west of the field (Fig. 7). The migrating wavy bedforms correspond to the sediment waves exhibited by the multibeam bathymetric data (Figs. 1 and 2). The coeval depositional sections of the sediment wave filed become thinner as close to the furrowed field and finally disappear due to the intense truncation of the sea floor (Fig. 7).

Oceanographic observations had been carried over 14 days at the Blake Outer Ridge (Stahr and Sanford, 1999). Three surveyed profiles at this study area were respectively located at the bathymetric profiles of p2, p3, and p5 in this study (Fig. 1b). The characteristics of the flow field related to the development of submarine furrows were illustrated by correlation of the bathymetric and corresponding oceanographic surveyed profiles (Fig. 8). All the three profiles across the zone of type A furrows show that a current with a significant abnormal speed flows south at up to 20 cm/s below the water depth of ~2000 m (Fig. 8). The current is considered to the DWBC (Stahr and Sanford, 1999). The sea bed where the submarine furrows appear basically matches the zone where the DWBC passes. Scatter plots of

Table 1 Furrow width, depth, spacing, and water depth identified from 12 cross-section bathymetric profiles. The locations of the bathymetric profiles are shown in Figure 1b.

Profiles	Width (m)			Depth (m)			Spacing (m)			Water depth (m			Width/spacing		
	Minum	Maximum	Mean	Minum	Maximum	Mean	Minum	Maximum	Mean	Minum	Maximum	Mean	Minum	Maximum	Mean
p1	154.7	1305.1	478.0	0.2	25.5	4.9	172.2	2568.9	619.9	3174.5	4382.3	3744.3	0.12	1.72	0.90
p2	189.3	1211.6	436.6	0.2	14.8	3.5	197.4	1313.7	474.5	2758.9	4520.9	3969.2	0.40	2.29	0.96
p3	67.2	1379.2	524.6	0.1	11.5	3.2	143.8	1878.7	611.8	3289.7	4528.5	4209.7	0.11	1.92	0.94
p4	250.5	1968.2	751.9	0.7	22.8	5.8	272.1	3043.6	935.5	3628.7	5050.2	4858.0	0.42	1.88	0.90
p5	153.1	2238.3	622.2	0.2	29.4	5.2	178.0	3019.1	823.3	3878.8	5386.2	5021.0	0.20	1.72	0.89
p6	169.2	1628.2	554.7	0.4	16.7	4.7	159.8	2021.1	655.5	4210.4	5187.4	4903.7	0.18	2.10	0.97
p7	233.1	1104.1	567.0	0.5	8.7	2.8	175.1	1928.6	805.8	2746.6	3150.4	3085.8	0.22	2.10	0.88
p8	115.3	1198.0	505.5	0.6	18.1	5.0	251.2	1168.1	616.7	3138.6	3209.4	3170.3	0.34	1.53	0.86
p9	341.1	1253.2	574.0	0.2	22.1	4.2	330.1	1635.1	739.8	3405.3	3689.8	3580.9	0.40	1.74	0.85
p10	263.4	1195.4	495.6	0.2	8.1	2.3	253.9	1862.1	691.7	3247.5	3709.9	3517.4	0.29	1.64	0.82
p11	354.8	1314.7	712.5	0.4	9.9	3.2	343.7	1989.5	828.6	3579.2	4449.6	4254.3	0.38	1.50	0.91
p12	291.5	1586.8	541.3	0.1	26.2	3.8	294.6	1538.9	681.3	3755.9	4503.7	4185.4	0.4	2.0	0.9

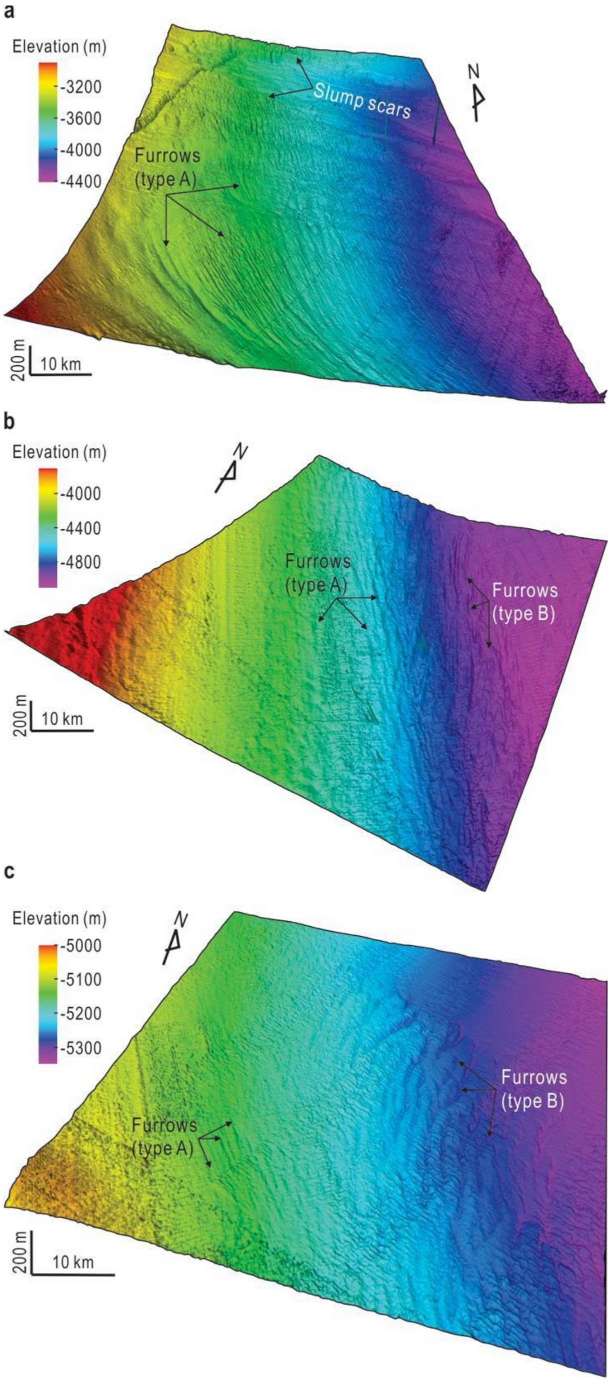

Fig. 3 Morphologic 3D-map view of three enlarged furrowed fields. Map locations 415 are shown in Figure 1b.

furrow spacing and flow speeds show a significant linearly proportional relationship between furrow spacing and speeds of the DWBC with a 0.97 linear coefficient (Fig. 9).

5. DISCUSSION

5.1. *ORIGIN OF THE SUBMARINE FURROWS*

Three major models have been proposed for the formation of submarine furrows, which are the obstacle blocking model (McLean, 1981), the flow filament erosion model (Garcia et al. 2009), and the secondary helical flow model (Flood, 1981, 1983), respectively. The first model explains that the formation of submarine furrows is associated with the development of turbulent flows in the lee of an obstacle due to the blocking (McLean, 1981). The turbulent flows convergent and abrade the sea bed, which finally produce furrows. The second model interprets that submarine furrows are related to erosion by the flow filaments separated from the mean flows (Garcia et al. 2009) or by bottom currents above pockmarks (León et al., 2010; Kilhams et al., 2011). The third model advocates that the formation of submarine furrow is related to the action of the secondary flow (Flood, 1981, 1983). When the current sweeps the sea bed, a secondary helical flow will be produced above the sea bed due to friction dag of the sea floor. The secondary flow cells form multiple convergent zones on the sea bed where the current is strengthened. The enhanced secondary flows on the convergent zones form submarine furrows.

In the first model, the formation of submarine furrows needs blocking of obstacles. The multibeam bathymetric data in this study show that the sea floor of the furrowed field is generally flat and simple except for two large slump scars (Figs. 1, 2 and 3). Hence, the morphologic characteristics of the furrowed field don't coincide with those described by the first model. Furthermore, the clustered furrows in our case need multiple isolated blocking obstacles which haven't been found on the seafloor based on the multibeam bathymetric data. Thus, the first model could be excluded.

The second model usually forms isolated furrows associated with location and number of flow filaments or pockmarks, which does not agree with the clustered elongated furrows in our case. The multibeam bathymetric data show no distinct pockmarks on the seafloor as well as the seismic data in the west of the furrow field (Figs. 1, 2, 3, 7). In addition, the furrows created in this model are similar to valleys and small contourite channels in size (Garcia et al., 2009; León et al., 2010; Kilhams et al., 2011) and are much larger than those in this study. Therefore the second model can hardly explain the origin of the furrows at the Blake Outer Ridge.

The third model could explain the formation of the submarine furrows in this study mainly based on the following reasons. (1) Oceanographic observations found the bottom boundary layer above the sea bed of the furrowed field which is necessary for the development of the secondary flow. Observations show a special water layer with a thickness of ~50 m above the sea bed characterized by decreasing flow speed with depth due to the friction of the sea floor (Stahr and Sanford, 1999). Turbulent kinetic energy dissipation rate in the bottom boundary layer is several

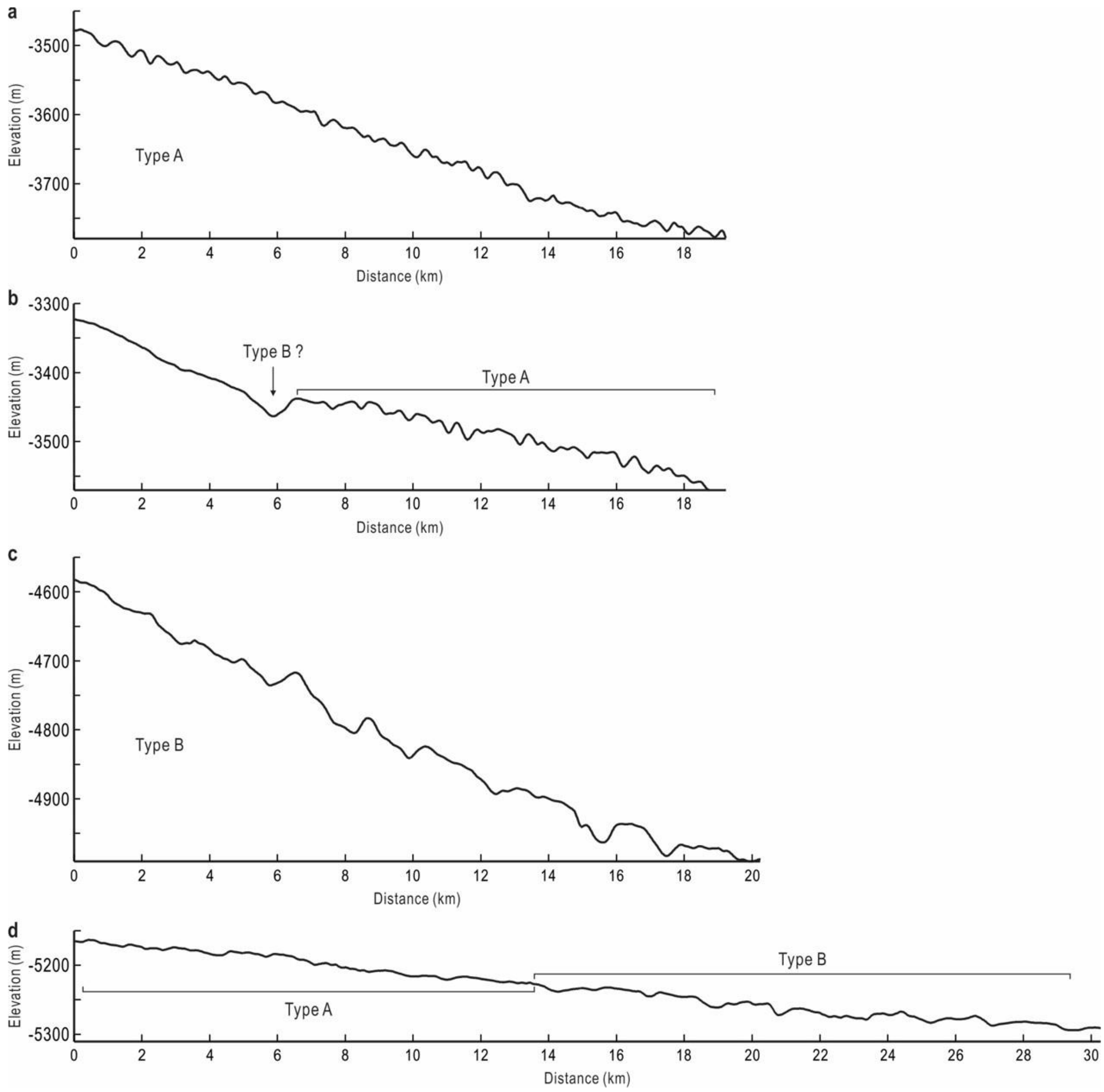

Fig. 4 Cross-section bathymetric profiles of c1–c4 that respectively correspond to (**a**) –(**d**). Profile locations are shown in Figure 1b.

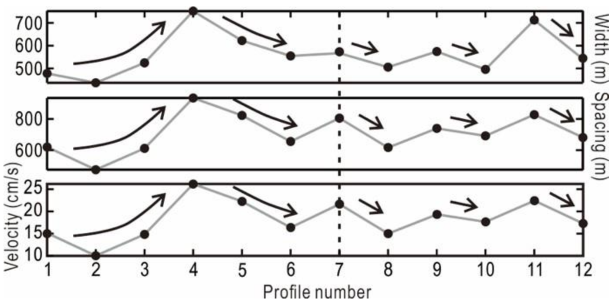

Fig. 5 Plots of average width (upper) and spacing (middle) of the furrows, and estimated mean velocity (lower) at the p1–p12 bathymetric profiles. Profile locations are shown in Figure 1b.

orders of magnitude larger than the mean flow as a result of increased turbulent mixing. The bottom boundary layer is distributed over the entire lines (Stahr and Sanford, 1999). (2) Observations documented the presence of helical flows within the bottom boundary layer. The oceanographic measurement at the bottom of the Lake Superior found the existence of streamwise, helical, counterrotating vortexes in the bottom boundary layer of a large natural body of waters (Viekman et al., 1989). (3) ODP sites 994, 995, 997 close to the furrowed field revealed that the sea bed mainly consists of fine-grained clays (Matsumoto et al., 1996) which favor abrasion of the secondary helical flows on the sea bed. (4) The flow velocity of the DWBC is large enough to form submarine furrows. Submarine furrows have been observed where bottom currents often flow at 5–20 cm/s

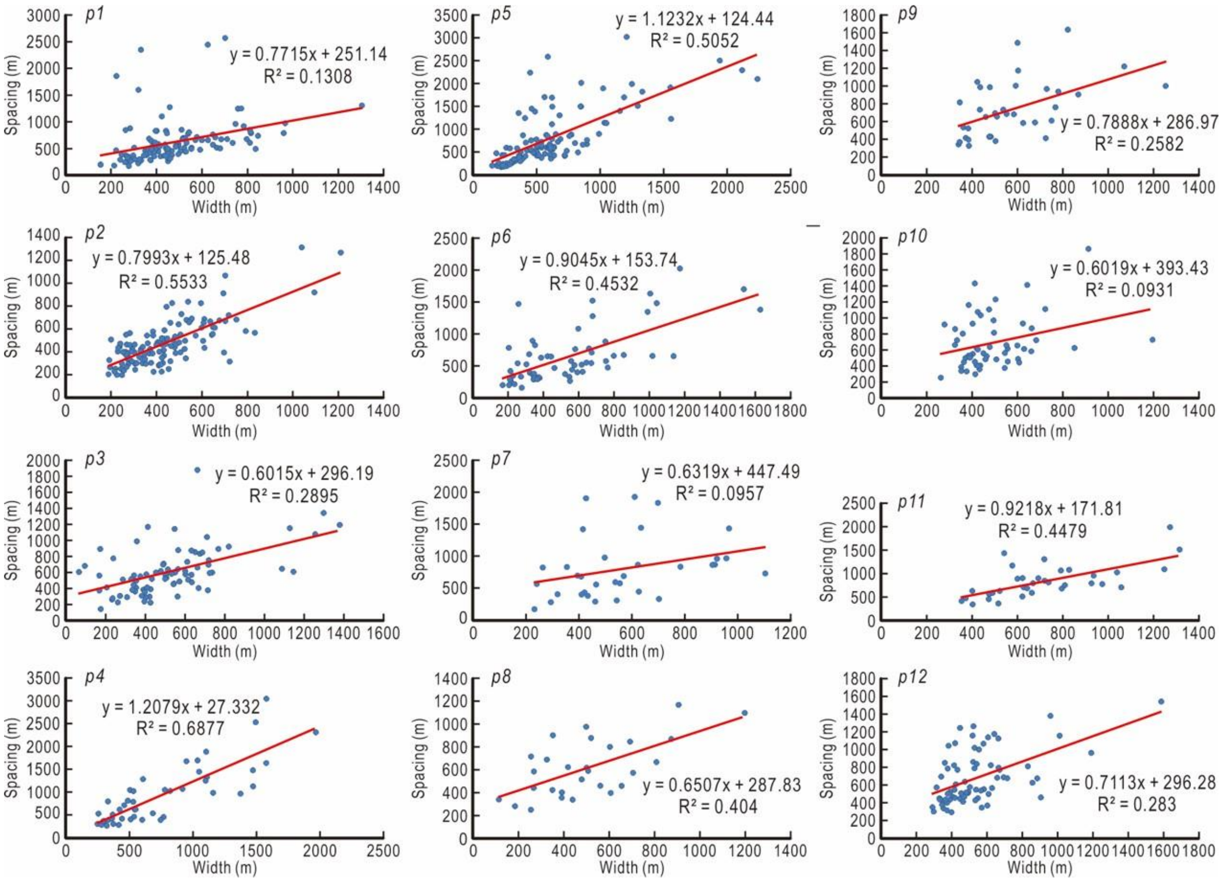

Fig. 6 Plots of furrow width to spacing collected from the p1–p12 bathymetric profiles. Blue dots represent the samples and red lines mark the trendlines. Profile locations are shown in Figure 1b.

(Flood, 1983). Oceanographic observations in this study area recorded 10–20 cm/s velocity of the long-term DWBC at the present environment (Stahr and Sanford, 1999). (5) The proportional relationship between furrow spacing and the mean flow speeds of the DWBC in this study matches the observation and principles of the secondary helical flows in the bottom boundary layer. Both the observations and theory indicate that the velocity of the mean flow is proportional to that of the secondary flow (Brown, 1970, 1980; Viekman et al., 1989) which is proportional to its diameter (equal to furrow spacing). Therefore the velocity of the mean flow should be proportional to furrow spacing.

In short, the submarine furrows at the Blake Outer Ridge have been formed by abrasion of the secondary helical counterrotating circulation in the bottom boundary layer of the DWBC (Fig. 10). In addition, oceanographic observations inside and outside of the study area indicated that the furrows of type A are functional or active features at the present (Flood, 1994; Stahr and Sanford, 1999).

5.2. EVOLUTION OF SUBMARINE FURROWS

Seismic data close to the west boundary of the furrowed field reveal that erosional processes probably dominated the sea bed on a long time scale inside the furrow field and depositional processes dominated the sea floor outside the furrow field (Fig. 7). V-shaped cross-sections of the furrows (Fig. 4) also imply that erosive flows responsible for the long-term development of the furrows. So, the furrows in this study probably represent an erosional feature.

Distinct differences between size, trend, and water depth of the type A and B furrows means different development stages of the furrows and various activity of the associated DWBC. The larger furrows of type B at a deeper water depth imply the stronger DWBC than that at the present. Previous studies suggested that the DWBC became stronger during Younger Dryas (cold climate) based on cores at 3720 and 4770 m water depths (Flood, 1994). Previous research also indicated the stronger DWBC with a shallower speed core during glacial periods (Oppo and Lehman, 1993; Franz and Tiedemann, 2002;

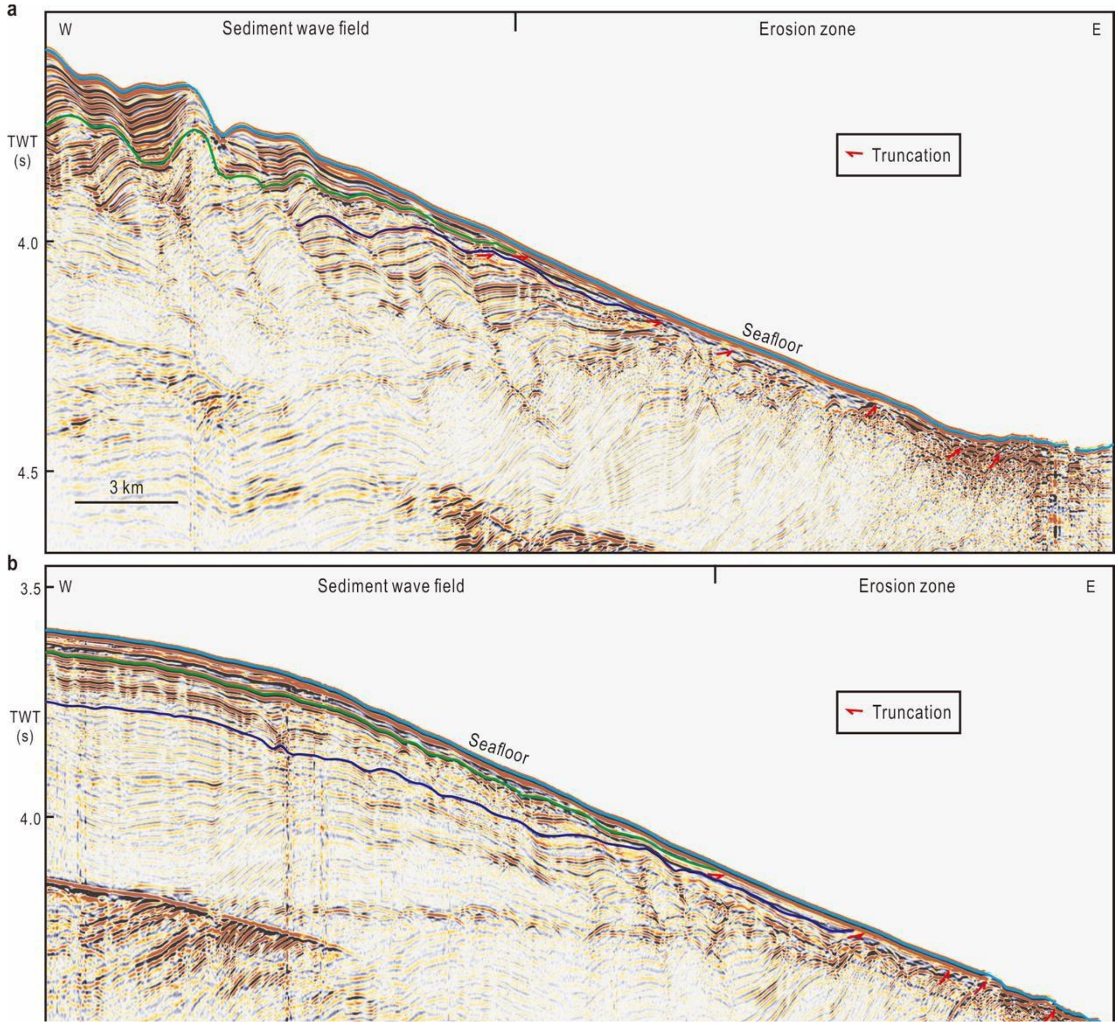

Fig. 7 Seismic profile in line1 (**a**) and in line 92 (**b**) showing depositional and erosional characteristics of the region close to the furrowed field. The light blue, green, and navy blue lines mark the seismic reflectors. Profile locations are shown in Figure 1b.

Evans and Hall, 2008). Hence, the evolution of the furrows at the Blake Outer Ridge could include two stages. During periods (e.g. glacial periods) when the DWBC is vigorous, the stronger bottom current abraded the sea bed and formed more erosional and larger furrows (type-B furrows in this study) at a larger water depth range by the secondary helical circulation in the bottom boundary layer (Fig. 10a). During periods (e.g. interglacial periods) when the DWBC is weak, the weakened bottom current swept the sea bed and created less erosional and smaller furrows (type- A furrows in this study) at a smaller water depth range by the secondary helical circulation (Fig. 10b).

5.3. IMPLICATIONS FOR SPATIAL VARIATIONS OF THE DWBC VELOCITY

The spatial variations of the DWBC velocity could be inferred according to the statistically derived linear relationship between furrow spacing and the DWBC velocity. Furrow spacing and average width firstly decrease toward the south, then increase significantly and reach maximum along the DWBC, indicating corresponding spatial changes of the DWBC velocity. The velocity of the DWBC firstly decreases toward the south, then significantly increases at a bend, and finally decreases gradually (Fig. 5). The velocity of all the three branches of the DWBC gradually decreases toward the west.

The DWBC velocity at any given location of the furrowed filed could be estimated according to the fitted quantitative relationship between furrow spacing and the DWBC velocity (Fig. 11). The significant decrease of the DWBC velocity from the profile p1 to profile p2 might attribute to the development of the southern slump scar (Figs. 5 and 11). This large scar might increase the roughness and friction of the sea bed therefore leads to rapid kinetic

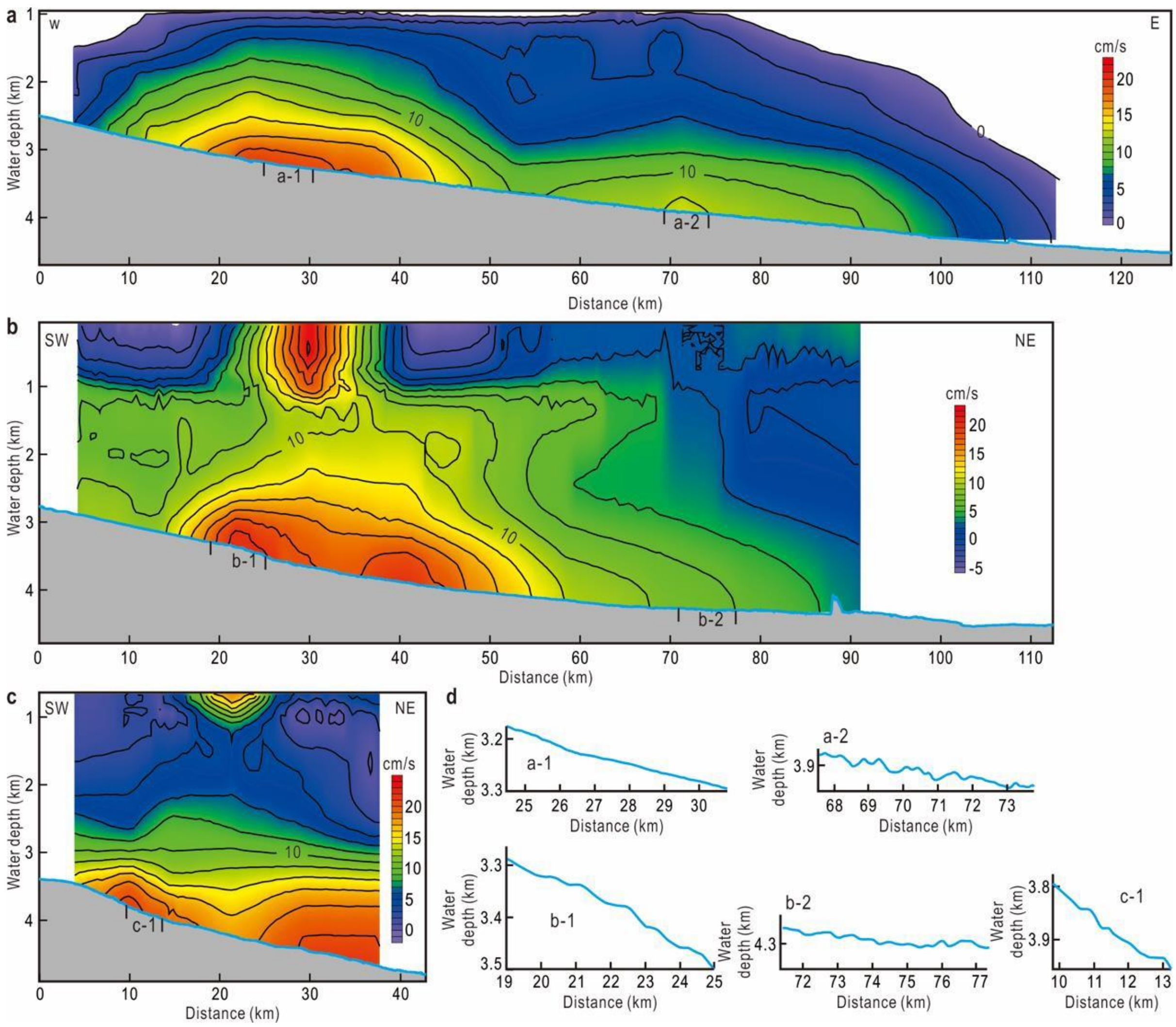

Fig. 8 Contours of geostrophic velocity normal to the profile sections of p2 (**a**), p3 (**b**), and p5 (**c**) (modified from Stahr and Sanford (1999)) and corresponding bathymetric profiles. Enlarged bathymetric profiles in the three long bathymetric profiles also shown in (**d**). Contour intervals are every 2 cm/s. The positive flow is equatorward. Profile locations are shown in Figure 1b.

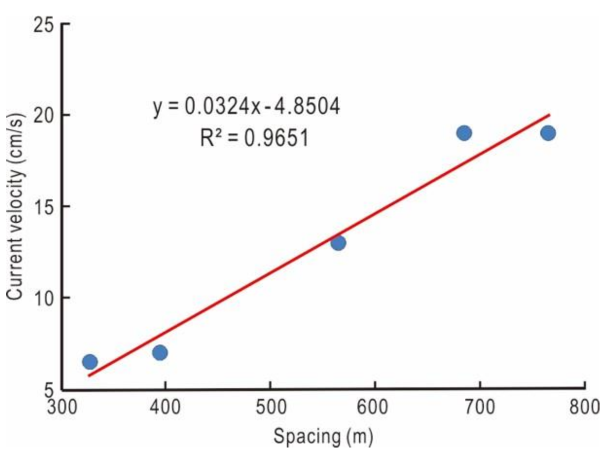

Fig. 9 Correlation of the flow velocity and furrow spacing based on statictis. Blue dots represent the 5 samples in Figure 8d and red lines mark the trendlines.

energy loss. It is notable that the DWBC velocity has more than doubled from the profile p2 to profile p4 (Fig. 5). All the three profiles (p2–p4) are located at a topographic bend, implying that the increase of velocity likely linked to the effect of topography (Fig. 11). When the DWBC flows south through the bend, the current would converge due to the blocking and confinement of the topography on the left side of the flow. Based on flux conservation assumption (e.g. Komar, 1973), the flow velocity would increase.

6. CONCLUSIONS

(1) A large furrowed field with ~83000km^2 has been developed at the Blake Outer Ridge in the U.S. Atlantic margin. The submarine furrows appear in clusters on the continental rise with a gradient of 0.43–0.62° at a water depth of 3000–5000 m where no distinct large gravity flow features (e.g. submarine canyons/channels and slump scars) have been developed. Most of them run along isobaths and a few

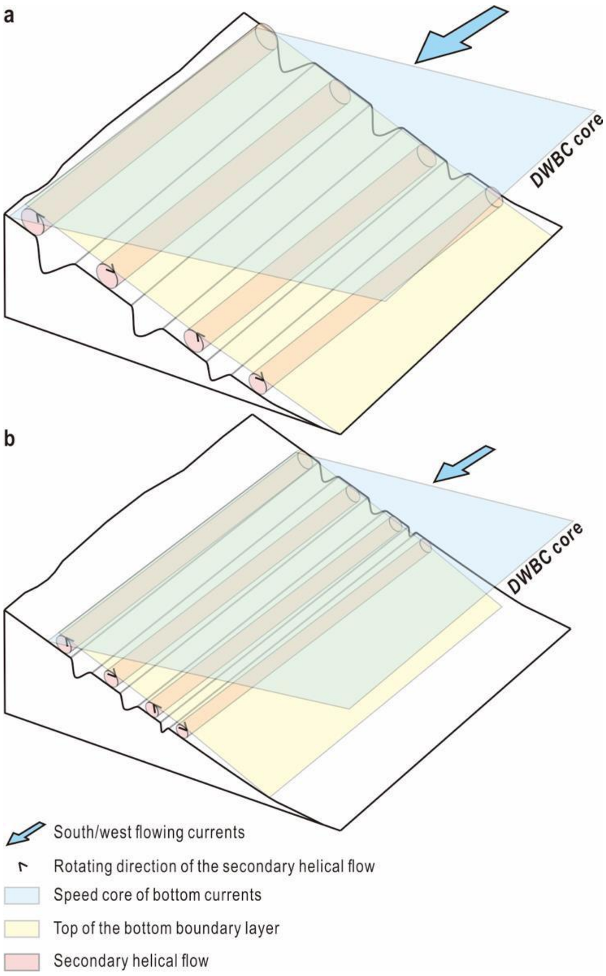

Fig. 10 Conceptual model illustrating submarine furrows at the Blake Outer Ridge governed by the vigorous (**a**) and weak (**b**) DWBC.

extends obliquely to the continental rise to ~30° at a deeper water depth. These furrows show asymmetric V-shaped cross-sections with a bit steeper walls on the upslope. They are 70–1100 m wide and 0.2–30 m deep. Furrow spacing varies between 145–3045 m. The average ratio of width to spacing is ~0.9. Statistics show a fine linear proportional relationship between the furrow width and spacing.

(2) Origin of the submarine furrows was related to the erosional processes of the along-slope DWBC. When the DWBC swept the sea bed from north to south, the secondary helical counterrotating flow in the bottom boundary layer of the mean flow created multiple convergent zones where the flow was strengthened and abraded the sea bed, resulting in the origin of the furrows with a certain spacing.

(3) The development of the furrows has been governed by the behavior of the DWBC. During periods (e.g. glacial periods) when the DWBC is vigorous, the stronger bottom current abraded the sea bed and formed more erosional and larger furrows at a larger water depth range. During periods (e.g. interglacial periods) when the DWBC is weak, the weakened bottom current swept the sea bed and created less erosional and smaller furrows at a smaller water depth range.

(4) The spatial variations of the DWBC velocity were estimated at the Blake Outer Ridge according to the statistically derived linear relationship between furrow spacing and the DWBC velocity. The DWBC generally flows at 10–30 cm/s, and the flow velocity decreases gradually along its path. But, the flow velocity had more than doubled through a bend and decreased by 1/3 across a large slump scar.

ACKNOWLEDGMENTS

This study is partly supported by National Key Research and Development Program of China (No. 2019YFB1600700). We are grateful to the National Oceanic and Atmospheric Administration (NOAA) for providing the open multibeam bathymetric data. We also thank Opendtect Corporation for offering the open seismic reflection data.

REFERENCES

Biscara, L., Mulder, T., Gonthier, E., Cremer, M., Faugères, J.-C. and Garlan, T.: 2010, Migrating submarine furrows on Gabbonese margin (West Africa) from Mioeene to present: Influence of bottom currents. Geo-Temas, 100, 21–22.

Bras, I.A.L., Yashayaev, I. and Toole, J.: 2017, Tracking Labrador Sea Water property signals along the Deep Western Boundary Current. J. Geophys. Res., Oceans, 122, 5348–5366. DOI: 10.1002/2017JC012921

Brown, R.A.: 1970, A Secondary Flow Model for the Planetary Boundary Layer. J. Atmos. Sci., 27, 742–757. DOI: 10.1175/1520-0469(1970)027

Brown, R.A.: 1980, Longitudinal instabilities and secondary flows in the planetary boundary layer: A review. Rev. Geophys., 18, 683–697.

Bryan, G.M.: 1970, Hydrodynamic model of the Blake Outer Ridge. J. Geophys. Res., 75, 4530–4537. DOI: 10.1029/JC075i024p04530

Canals, M., Puig, P., de Madron, X.D., Heussner, S., Palanques, A. and Fabres, J.: 2006, Flushing submarine canyons. Nature, 444, 354–357. DOI: 10.1038/nature05271

Dyer, K.R.: 1970, Linear erosional furrows in Southampton Water. Nature, 225, 56–58. DOI: 10.1038/225056a0

Evans, H.K. and Hall, I.R.: 2008, Deepwater circulation on Blake Outer Ridge (western North Atlantic) during the Holocene, Younger Dryas, and Last Glacial Maximum. Geochem. Geophys. Geosystems, 9, 680–680. DOI: 10.1029/2007GC001771

Faugères, J.C., Stow, D.A.V., Imbert, P. and Viana, A.: 1999, Seismic features diagnostic of contourite drifts. Mar. Geol., 162, 1–38. DOI: 10.1016/S0025-3227(99)00068-7

Flood, R.D.: 1981, Distribution, morphology and origin of sedimentary furrows in cohesive sediments, Southampton Water. Sedimentology, 28, 511–529. DOI: 10.1111/j.1365-3091.1981.tb01699.x

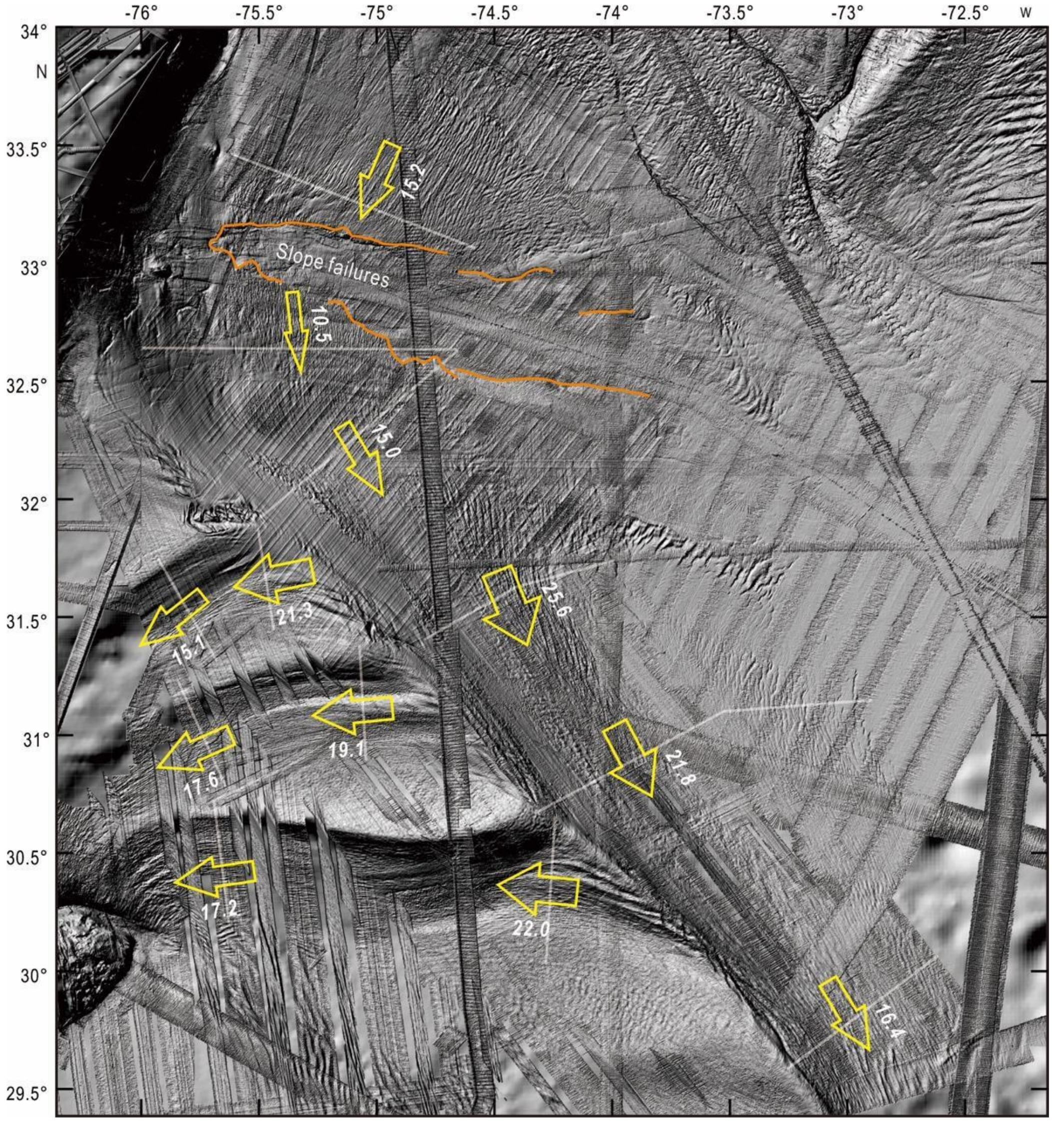

Fig. 11 Spatial variations of the DWBC velocity estimated from the correlation of the furrow spacing and the flow velocity. Yellow arrows mark the flow direction. Orange lines mark slump scars. Translucent white lines represent the locations of the p1–p12 bathymetric profiles. White numbers nearby yellow arrows denote flow velocity with a unit of cm/s.

Flood, R.D.: 1983, Classification of sedimentary furrows and a model for furrow initiation and evolution. Geol. Soc. Am. Bull., 94, 630–639. DOI: 10.1130/0016-606(1983)94

Flood, R.D.: 1994, Abyssal bedforms as indicators of changing bottom current flow: Examples from the US East Coast continental rise. Paleoceanography, 9, 1049–1060. DOI: 10.1029/94PA01801

Franz, S.O. and Tiedemann, R.: 2002, Depositional changes along the Blake–Bahama Outer Ridge deep water transect during marine isotope stages 8 to 10 – links to the Deep Western Boundary Current. Mar. Geol., 189, 107–122. DOI: 10.1016/S0025-3227(02)00325-0

García, M., Hernández-Molina, F.J., Llave, E., Stow, D.A.V., León, R., Fernández-Puga, M.C., Del Río, V.D. and Somoza, L.: 2009, Contourite erosive features caused by the Mediterranean Outflow Water in the Gulf of Cadiz: Quaternary tectonic and oceanographic implications. Mar. Geol., 257, 1-4, 24–40. DOI: 10.1016/j.margeo.2008.10.009

Hornbach, M.J., Saffer, D.M., Holbrook, W.S., Van Avendonk, H.J. and Gorman, A.R.: 2008, Three-dimensional seismic imaging of the Blake Ridge methane hydrate province: Evidence for large, concentrated zones of gas hydrate and morphologically driven advection. J. Geophys. Res., Solid Earth, 113, B07101. DOI: 10.1029/2007JB005392

Jenkins, W.J. and Rhines, P.B.: 1980, Tritium in the deep north Atlantic Ocean. Nature, 286, 877–880. DOI: 10.1038/286877a0

Kilhams, B., McArthur, A., Huuse, M., Ita, E. and Hartley, A.: 2011, Enigmatic large-scale furrows of Miocene to Pliocene age from the central North Sea: current-scoured pockmarks. Geo-Mar. Lett., 31, 437–449. DOI: 10.1007/s00367-011-0235-1

Komar, P.D.: 1973, Continuity of turbidity current flow and systematic variations in deep-sea channel morphology. Geol. Soc. Am. Bull., 84, 3329–3338. DOI: 10.1130/0016-7606(1973)84

Lastras, G., Canals, M., Urgeles, R. et al.: 2007, A walk down the Cap de Creus canyon, Northwestern Mediterranean Sea: Recent processes inferred from morphology and sediment bedforms. Mar. Geol., 246, 176–192. DOI: 10.1016/j.margeo.2007.09.002

Lobo, F.J. et al.: 2011, Furrows in the southern Scan Basin, Antarctica: interplay between tectonic and oceanographic influences. Geo-Mar. Lett., 31, 451–464. DOI: 10.1007/s00367-011-0240-4

Lonsdale, P.F., Spiess, F.N. and Mudie, J.D.: 1973, Erosional furrows across the abyssal Pacific floor. Trans. Am. Geophys. Union, 54, 1110.

Lynch-Stieglitz, J., Curry, W.B. and Slowey, N.: 1999, Weaker Gulf Stream in the Florida Straits during the Last Glacial Maximum. Nature, 402, 644–648.

Lynch-Stieglitz, J., Schmidt, M.W. and Curry, W.B.: 2011, Evidence from the Florida Straits for Younger Dryas ocean circulation changes. Paleoceanography, 26, 97–107. DOI: 10.1029/2010PA002032

Matsumoto, R., Ryo, M.D., Paull, C., Fox, P.J., Francis, T.J., Wallace, P. and Baldauf, J.: 1996, Gas hydrate sampling on the Blake Ridge and Carolina Rise. Proc ODP, Initial Reports, College Station, TX (Ocean Drilling Program).

McLean, S.: 1981, The role of non-uniform roughness in the formation of sand ribbons. Mar. Geol., 42, 49–74. DOI: 10.1016/0025-3227(81)90158-4

Mosher, D.C., Campbell, D., Gardner, J., Piper, D., Chaytor, J. and Rebesco, M.: 2017, The role of deep-water sedimentary processes in shaping a continental margin: The Northwest Atlantic. Mar. Geol., 393, 245–259. DOI: 10.1016/j.margeo.2017.08.018

Oppo, D.W. and Lehman, S.J.: 1993, Mid-depth circulation of the subpolar north Atlantic during the last glacial maximum. Science, 259, 1148–1152. DOI: 10.1126/science.259.5098.1148

Phrampus, B.J. and Hornbach, M.J.: 2012, Recent changes to the Gulf Stream causing widespread gas hydrate destabilization. Nature, 490, 527–530. DOI: 10.1038/nature11528

Poppe, L., Knebel, H., Lewis, R. and DiGiacomo-Cohen, M.: 2002, Processes controlling the remobilization of surficial sediment and formation of sedimentary furrows in north-central Long Island Sound. J. Coast. Res., 18, 741–750.

Rebesco, M., Hernández-Molina, F.J., Van Rooij, D. and Wåhlin, A.: 2014, Contourites and associated sediments controlled by deep-water circulation processes: State-of-the-art and future considerations. Mar. Geol., 352, 111–154. DOI: 10.1016/j.margeo.2014.03.011

Stahr, F.R. and Sanford, T.B.: 1999, Transport and bottom boundary layerobservations of the North Atlantic Deep Western Boundary Current at the Blake Outer Ridge. Deep Sea Research Part II. Top. Stud. Oceanogr., 46, 205–243. DOI: 10.1016/S0967-0645(98)00101-5

Stow, D.A., Hernández-Molina, F.J., Llave, E., Sayago-Gil, M., …, Branson, A.: 2009, Bedform-velocity matrix: the estimation of bottom current velocity from bedform observations. Geology, 37, 327–330. DOI: 10.1130/G25259A.1

Stow, D.A.V. et al.: 2013, The Cadiz Contourite Channel: Sandy contourites, bedforms and dynamic current interaction. Mar. Geol., 343, 99–114. DOI: 10.1016/j.margeo.2013.06.013

Viekman, B.E., Flood, R.D., Wimbush, M., Faghri, M., Asako, Y. and Leer, J.C.: 1992, Sedimentary furrows and organized flow structure: A study in Lake Superior. Limnol. Oceanogr., 37, 797–812. DOI: 10.4319/lo.1992.37.4.0797

Viekman, B.E., Wimbush, M. and Leer, J.C.: 1989, Secondary circulations in the bottom boundary layer over sedimentary furrows. J. Geophys. Res., Oceans, 94, 9721–9730. DOI: 10.1029/JC094iC07p09721